

Ultra-broadband optical amplifiers for WDM

Yasutake OHISHI
 Toyota Technological Institute
 2-12-1 Hisakata, Tempaku, Nagoya 468-8511, JAPAN
 E-mail : ohishi@toyota-ti.ac.jp

ABSTRACT

The operational bandwidth of optical fiber amplifiers has been expanded by developing rare-earth-doped fiber amplifiers and fiber Raman amplifiers (FRA), aiming at realizing ultra-broadband optical amplifiers in this decade. Especially, non-silica-based rare-earth-doped fiber amplifiers have played an important role in opening up new amplification bands. This paper reviews a development status of optical fiber amplifiers.

Keywords: broadband amplifier, rare-earth-doped fiber amplifier, Raman amplifier, non-silica-based fiber

1. INTRODUCTION

The demand for the development of ultra-high capacity transmission systems using wavelength division multiplexing (WDM) technology has accelerated efforts to expand the usable bandwidth of optical transmission systems. Broadening and flattening the amplification bandwidth of EDFAs have been key issues in terms of increasing the transmission capacity of WDM transmission systems and all-optical self-routed wavelength-addressable networks. Several approaches have already been employed to broaden and flatten the EDFA gain spectrum. Techniques utilizing (1) filter-based gain equalization, (2) multi-stage configurations, (3) an EDFA and fiber Raman amplifier (FRA) in a cascade configuration, (4) parallel configurations of two amplification bands and (5) new host-based EDFAs have been developed with a view to realizing broad bandwidth EDFAs. Energetic efforts in the past decade have advanced the great progress in this field. Especially, the development of rare-earth-doped fiber amplifiers using new host materials has opened up new possibilities for optical fiber amplifier technology. FRA technology has made remarkable progress. Furthermore, the research of fiber optical parametric amplifiers (OPA) has made progress by developing high nonlinear fibers. Recent progress of optical fiber amplifier technology is reviewed in this paper.

2. TDFA TECHNOLOGY

2.1 Gain-shifted TDFA

It is known that the TDFA has a 1450-1480 nm operation band^{(1),(2)}. It has recently become necessary to shift this operation band to a longer wavelength in order to use the TDFA for WDM transmission applications. There are two ways to obtain a gain-shifted TDFA (GS-TDFA) that operates in the S-band (1480 - 1510 nm). One approach involves dual wavelength (1.4 and 1.56 μm) pumping⁽³⁾ and the other involves using a TDFA doped with a high concentration of thulium⁽⁴⁾. Another important technical issue related to TDFA development is to find a way to increase the power conversion efficiency (PCE) because the highest PCE yet demonstrated for a GS-TDFA is as low as 10 %⁽³⁾. The PCE has been improved by employing a high thulium concentration doping technique.

Figure 1 shows a simplified energy level diagram of thulium. There is a low population inversion between $^3\text{H}_4$ and $^3\text{F}_4$ due to the cross relaxation ($^3\text{H}_4 - ^3\text{F}_4$) - ($^3\text{H}_6 - ^3\text{F}_4$) transition. Signal gains at shorter wavelengths are depressed and those at longer wavelengths remain⁽⁵⁾. Energy matching between the 1.4 μm pump photon energy and the energy level intervals for excitation transitions is much better than with 1.0 μm pumping. Therefore, we

can expect a higher PCE to be achieved if we use 1.4 μm pumping. Figure 2 shows the TDF length dependence of the PCE for 1.4 and 1.0 μm pumping⁽⁵⁾. The concentration of the thulium doped in the core was 6000 ppm. The total

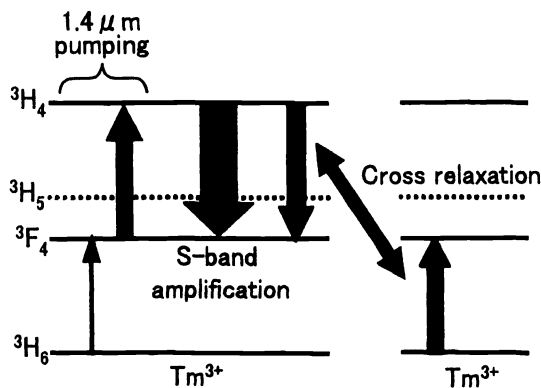


Figure 1 Energy diagram of thulium

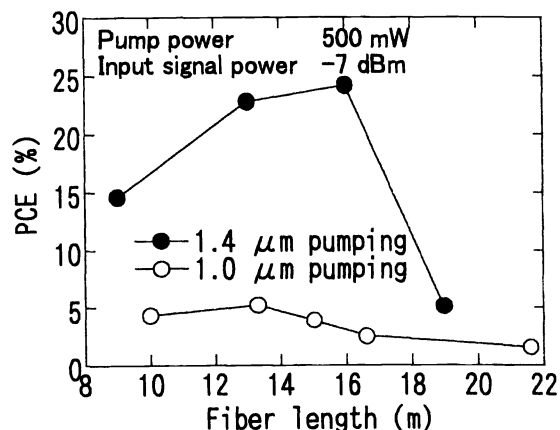


Figure 2 PCE dependence on fiber length

pump power was kept at 500 mW and the input signal power was -16 dBm/ch x 8 ch between 1481 and 1505 nm. The maximum PCE was 25 % when using 1.4 μm pumping, whereas it was 5 % for 1.0 μm pumping. The PCE obtained with 1.4 μm pumping is almost five times that obtained with 1.0 μm pumping.

Figure 3 shows the fiber length dependence of the PCE for GS-TDFAs with a single and double pass configuration⁽⁵⁾. The concentration of the thulium doped in the core was 6000 ppm. The pump power was 500 mW and the total input signal power was -7 dBm. When a longer fiber is used, the gain band shifts to a longer wavelength region. We must tune the TDF length as a function of the input signal power and pump power to realize the required S-band amplification performance. The double-headed arrows show the suitable fiber length regions for flat gain operation in the S-band region. It is found that the PCE with a double pass configuration is as much as 10 % higher than that with a single pass configuration when the TDF length is optimized.

Figure 4 shows the configuration of a GS-TDFA with a double pass configuration⁽⁵⁾. The 6000 ppm thulium doped TDFs in the first and second stages were 3 and 5 m long, respectively. A scanning probe method was used to evaluate the amplification performance in which saturation signals with a total power of -7 dBm and -30 dBm probe signals were input into the fiber.

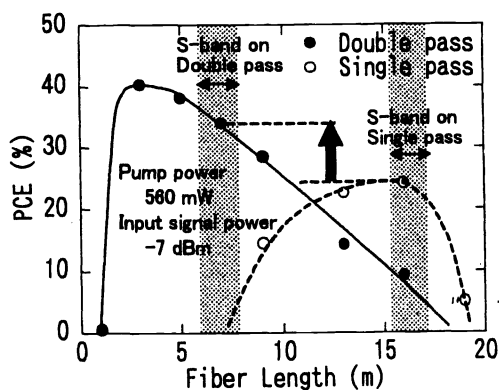


Figure 3 PCE for GS-TDFA dependence on fiber length

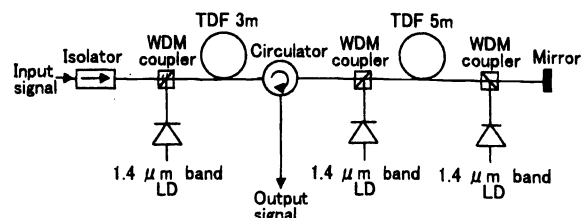


Figure 4 GS-TDFA configuration

Figure 5 shows the gain and noise figure spectra of this GA-TDFA⁽⁵⁾. The total pump power was 580 mW and the total input signal power was -7 dBm. The GS-TDFA had a gain of over 26 dB and noise figure of less than 7 dB in the 1480 - 1510 nm wavelength range. The output power was 23.9 dBm and the PCE was 42 %.

A 8 x 10 Gb/s WDM transmission experiment was performed using this GS-TDFA. Eight multiplexed signals (1483.86 - 1505.35 nm) were intensity modulated by using an LN modulator with a 10 Gb/s 2²³-1 pseudo random bit stream and amplified by a post GS-TDFA after passing through a 10 km long single-mode fiber. The boosted signals with a power level of 5 dBm/ch passed through a 120 km long DSF with a transmission loss of 30 dB. The transmitted signals were amplified by a pre-GS-TDFA and detected with a pin-PD receiver.

Figure 6 shows the bit error rate (BER) measured at the input position of the pin-PD⁽⁵⁾. Error free operation with a BER of 10⁻¹² was confirmed for all channels. The power penalties after transmission were mainly caused by transmission fiber dispersion and SNR degradation in the transmission system and were less than about 1.5 dB. There was no excess noise generated in the TDFAs with the double pass configuration except for the inherent signal-spontaneous beat noise.

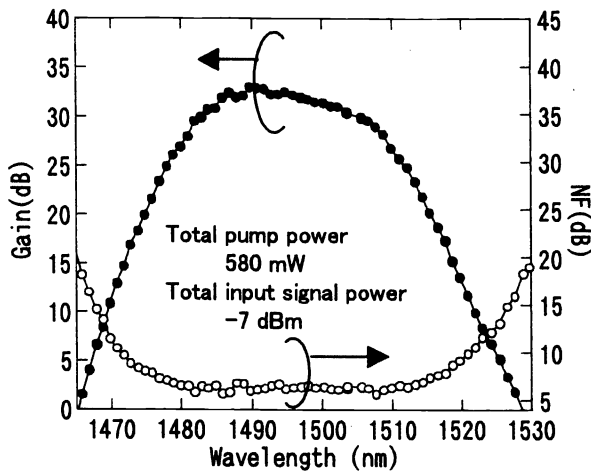


Figure 5 Gain and noise spectra of GS-TDFA

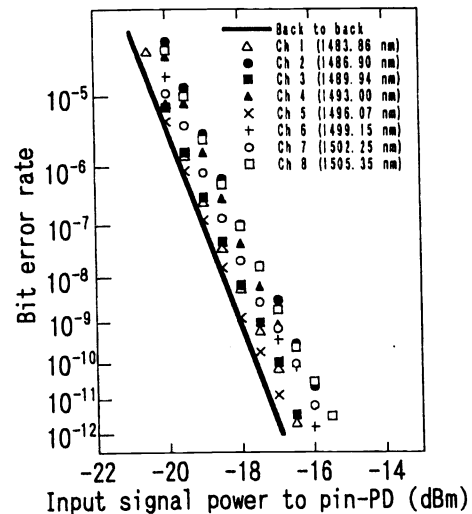


Figure 6 BER characteristics

Although GS-TDFAs have been demonstrated, their gain reduction is still too great for WDM applications at wavelengths longer than 1510 nm as described in the above section. Signal amplification in the 1510 - 1520 nm has been demonstrated using a fiber Raman assisted TDFA⁽⁶⁾. It has recently been shown that fiber Raman assisted EDFAs can operate in the 1488 - 1518 nm signal range⁽⁷⁾. Although a cascaded amplifier consisting of a silica-based EDFA (EDSFA) and silica-based TDFA has been demonstrated with a view to realizing rare-earth-doped fiber amplifiers that can operate in the S and C-bands, unfortunately its performance is insufficient for WDM signal amplification⁽⁸⁾. No rare-earth doped fiber amplifier has yet been demonstrated whose amplification performance makes it suitable for WDM signal amplification.

Fluoride-based TDF and silica-based EDF (EDSF) have been used to extend the amplification bandwidth of conventional TDFAs to a longer wavelength range, namely the 1510-1520 nm range. The fiber amplifier demonstrated in the experiment included two EDSFs and TDF as amplification media. The product of the fiber length and dopant concentration was 2,000 and 10,000 ppm·m for the two EDSFs and 80,000 ppm·m for the TDF. The fibers were connected in series. The optical signal was first amplified by the first EDSF and then amplified by the TDF. And finally, it was amplified by the second EDSF. The EDSF and TDF were pumped at 0.98 and 1.40 μm, respectively. The pump power was 138 mW for the first EDSF, 270 mW for the second EDSF and 240 mW for

the TDSF.

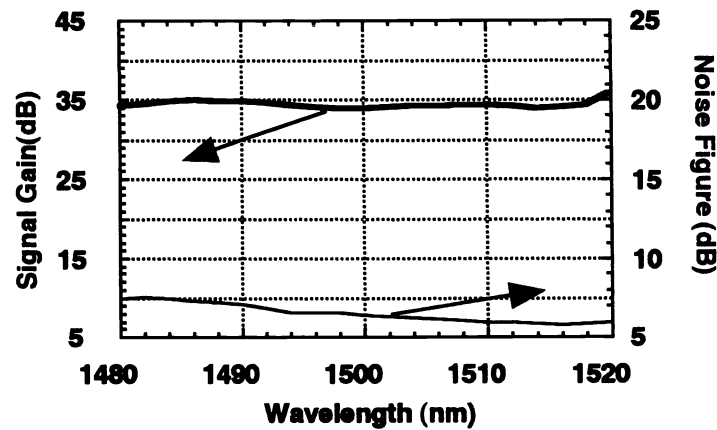


Figure 7 Gain and noise figure spectra of extended GS-TDFA

Figure 7 shows the signal gain and noise figure spectra for this fiber amplifier. The input signal level was -30 dBm. Small signal gains over 30 dB were obtained in the 1460 to 1560 nm wavelength range. Flattened gain was obtained in the 1480 to 1520 nm range where a TDFA cannot operate with sufficiently high gain and there is a valley in the TDFA and EDFA gain spectra as shown in Fig. 7. The noise figure was less than 7.5 dB at wavelengths shorter than 1480 nm. EDFAs can operate with sufficiently low noise figures even at wavelengths shorter than 1520 nm, if the population inversion between the $^4I_{15,2}$ and $^4I_{13,2}$ level is kept sufficiently high. In contrast, the TDFA noise figure increases greatly at wavelengths longer than 1510 nm due to the effect of the 3H_6 to 3F_4 ground state absorption. The TDFA operation range has been limited to wavelengths shorter than 1510 nm. However, the intrinsic impairment of the TDFA noise figure was overcome by this demonstrated serial amplification configuration with EDSF and TDF.

3. EDTFA TECHNOLOGY

We have investigated fiber host materials that are capable of realizing an intrinsically broader gain bandwidth than those of silica and fluoride-based EDFs. We have selected glass hosts with high refractive indices as broadband erbium hosts, because the stimulated emission cross-section (σ) due to the electric dipole moment transition of rare earth ions increases as the refractive indices of the hosts increase ($\sigma \sim (n^2+2)^2/n$)^(9,10) and as a result, it becomes possible to obtain amplification gain over a broader wavelength range than with low refractive index hosts. From this point of view, tellurite glass is advantageous in terms of enhancing the stimulated emission cross-section because its refractive index is over 2.

The longer operational wavelength limit of EDFAs is determined by the relation between the $^4I_{13,2} - ^4I_{15,2}$ stimulated emission and $^4I_{13,2} - ^4I_{9,2}$ excited state absorption (ESA) cross-section spectra. Figure 8 shows the $^4I_{13,2} - ^4I_{15,2}$ stimulated emission and the $^4I_{13,2} - ^4I_{9,2}$ ESA cross-section spectra in the longer wavelength region of erbium doped in tellurite, fluoride and silica glass⁽¹¹⁾. The inset shows the whole stimulated emission spectra for erbium in the three glasses. The stimulated emission cross-section of erbium in tellurite glass is larger than that in fluoride and silica glass over the whole spectral range, and is almost double those for fluoride and silica glass around 1.6 μm . This indicates that it is easy to obtain larger amplification gains around 1.6 μm if tellurite-based fiber is used as the erbium host.

The intersection of the emission and ESA cross-section spectra corresponds to the longer operational wavelength limit of EDFAs. Signal gain cannot be obtained at wavelengths longer than the intersection

wavelength. The intersection for erbium in tellurite was obtained at 1637 nm. By contrast, those for silica and fluoride glass were 1628 and 1630 nm, respectively. The operational wavelength range of the EDTFA is expected to extend 7 to 9 nm further into the longer wavelength region than silica or fluoride-based EDFAs.

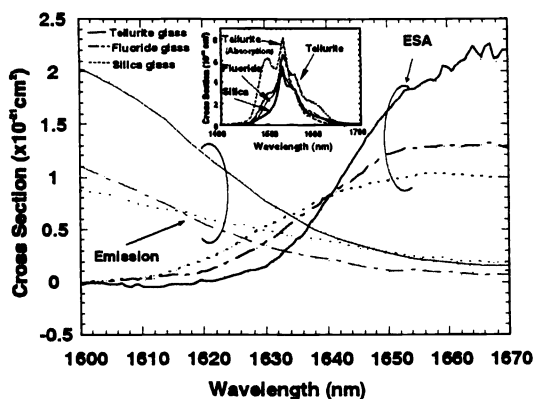


Figure 8 Emission and ESA cross section spectra of erbium in tellurite glass

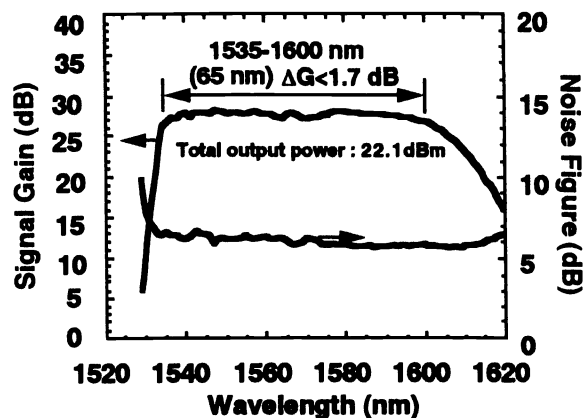


Figure 9 Gain and noise figure spectra of a gain flattened EDTFA

3.1 Broadband EDTFA operation

Figure 9 shows the gain and noise figure spectra of a gain flattened EDTFA. This broadband EDTFA consists of three stages. The 1000 ppm erbium doped EDTFs in the first, second and third stages were 2, 3 and 2.4 m long, respectively. The Δn and cutoff wavelength were 1.5 % and 1.4 μm , respectively. Two gain equalizers (GEQ) were inserted between the first and second, and the second and third stages, respectively, to achieve gain equalization and a large output power simultaneously. Each EDTF was pumped with 1.48 μm -LDs. A scanning probe method was used to evaluate the amplification performance by inputting saturation signals with a total power of -5 dBm (8 x -14dBm/ch) and -30 dBm probe signals.

An average signal gain in the 1535 - 1600 nm band was 27.1 dB and the excursion was 1.7 dB. The signal output power was 22.1 dBm. The noise figure was less than 7 dB in this band. By using EDTFs, a broadband gain flattened EDFA was realized that could cover the C and L-bands.

3.2 L-band EDTFA operation

The L-band EDSFA has a practical advantage in that its gain non-uniformity is less than 1 dB without gain equalizers in the 1570 to 1600 nm wavelength range. When the gain bandwidth is expanded over 1600 nm, the EDSFA has a large gain non-uniformity to complement the small gain efficiency above 1600 nm and therefore requires a large amount of gain equalization. A great advantage of the EDTFA is that it has larger gain efficiency than the EDSFA at wavelengths over 1600 nm. The EDTFA is a suitable amplifier with which to expand the gain bandwidth of the L-band EDFA. Here, the amplification characteristics of the L-band EDTFA are described.

Figure 10 shows the gain and noise figure spectra of the EDTFA and EDSFA⁽¹²⁾. The gain characteristics were measured by scanning the gain bandwidth with a -30 dBm probe signal while eight WDM signals (1570-1598 nm, equally spaced at 4 nm) were input at a power of -16.3 dBm/ch. The EDTF and EDSF were 11 and 180 m long, respectively. The pump power was adjusted so that flat gain spectra were obtained. The respective 3 dB-down gain bandwidths for the EDTFA and EDSFA were 50 nm (1560 - 1610 nm) and 38 nm (1568 - 1606 nm) with a peak gain of 29 dB. The difference between the PCE of the L-band EDTFA and EDSFA was as small as 1 - 2 % and the actual PCE of the EDTFA was 48 - 62 % depending on the pumping condition.

Figure 11 shows the gain and noise figure spectra of a gain flattened L-band EDTFA⁽¹²⁾. The gain characteristics of this L-band EDTFA were measured by sweeping a -30 dBm probe signal over the L-band while eight WDM signals (1561 - 1610 nm equally spaced at 7 nm) were input at a power of -14 dBm/ch. This amplifier consists of two amplifier units, and a GEQ is inserted between the two units. The first and second units were forward and backward pumped by 1.48 μm LDs, respectively. The EDTF was doped with erbium (1000 ppm) and its cutoff wavelength and refractive index difference were 1.4 μm and 1.5 %, respectively. An average gain of 25.3

dB with a slight gain excursion of 0.6 dB and a noise figure of less than 6 dB were obtained over a broad bandwidth

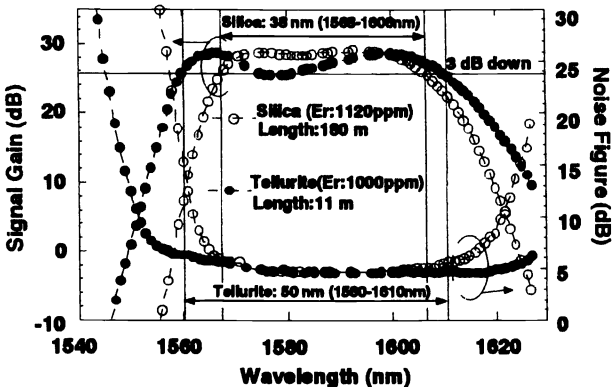


Figure 10 Gain and noise figure spectra of L-band EDTFA and EDSFA

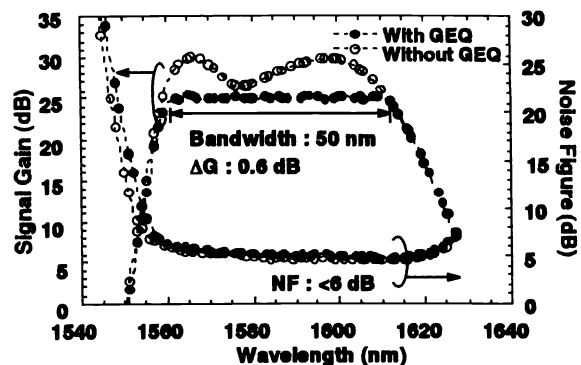


Figure 11 Gain and noise figure spectra of a gain flattened L-band EDTFA

of 50 nm in the 1561 – 1611 nm region. The total signal output power was 20.4 dBm and the PCE was 32.8 %, which is a practical value for high capacity WDM transmission applications.

It is difficult for EDSFAs to provide WDM signals with sufficient gain at wavelengths over 1600 nm. This is because the stimulated emission cross-section of EDSAFs becomes small at wavelengths over 1600 nm and their noise figure starts to increase at around 1610 nm due to signal excited-state absorption (ESA). EDTFAs are advantageous in that they have a large emission cross-section above 1600 nm and their noise figure increases above 1620 nm. It is advantageous to use EDTF when we expand the operational band of EDFAs towards the longer wavelength range.

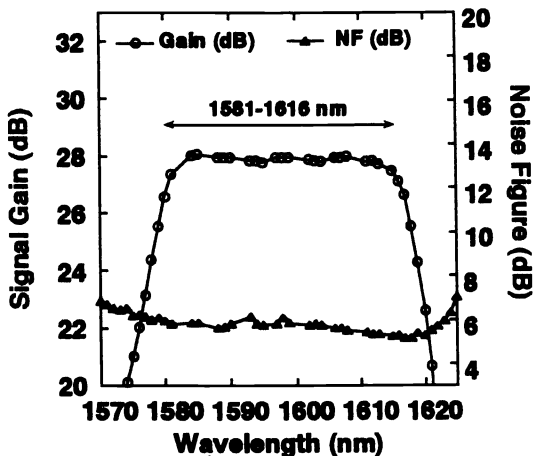


Figure 12 Gain and noise figure spectra of gain-shifted L-band EDTFA

Table 1 Fiber parameters of EDTFs and EDSFs

Sample	Amplifier	MFD (μm)	Er (ppm)	Cutoff (μm)	EDF length for 25.5dB gain (m)
A	EDTFA	3.5	1000	1.4	14
B	EDTFA	5	1000	1.4	11
C	EDTFA	7.5	1000	1.4	10
D	EDTFA	7.5	2000	1.4	5.4
E	EDSFA	5	1000	0.9	200
F	EDSFA	5	1000	1.4	36

Figure 12 shows the signal gain and noise figure spectra of a gain-shifted L-band EDTFA⁽¹³⁾. The EDTFA consists of two amplification units and a GEQ is inserted between the two amplification units. The erbium concentration was 1000 ppm and Δn was 1.5 %. The cutoff wavelength was 1.4 μm. The two EDTFs were each 9 m long. The GEQ was constructed from three cascaded Fabry-Perot etalon filters. Eight WDM signals equally spaced at 4.5 nm from 1582.5 to 1614 nm were launched into the EDTFA at a power of -16.5 dBm/ch. The total input power was -7.5 dBm. A -30 dBm probe signal was input into the EDTFA with the eight channel WDM

signals, when the gain and noise figure spectra were measured. When the pump powers of the first unit and the forward and backward pumping 1.48 μm -LDs of the second unit were 140, 150 and 175 mW, respectively, an average gain of 28 dB was obtained with a gain excursion of 1 dB and a noise figure of less than 6 dB over a bandwidth of 35 nm in the 1581 - 1616 nm wavelength range. The total output power of the eight WDM signals was 20.5 dBm. The power conversion efficiency of this gain flattened EDTFA reached 25 %. The operational bandwidth of the L-band EDFA was extended to 1616 nm by using an EDTFA. EDTFAs are effective for broadening the amplification band in the L-band range.

3.3 Four-wave mixing performance in EDTFAs

There has been concern that the nonlinear effects of, for example, four-wave mixing (FWM) and cross-phase modulation (XPM), on transmission quality would be more serious in EDTFAs than in EDSFAs because tellurite-based glass has large nonlinear coefficients. Even the nonlinear phenomena generated in EDSFAs, especially when they are operated in the L-band, have an adverse influence on transmission quality. One easy method of suppressing these nonlinear phenomena is to increase the mode field diameter and shorten the EDF length. Here, FWM which occurs in EDTF, is compared with that in EDSF and it is shown that it can be suppressed by choosing the fiber parameters.

Table 1 lists the fiber parameters of tellurite and silica-based EDFs for comparison⁽¹⁴⁾. The lengths of all the EDFs were adjusted so that the gain was around 25.5 dB when the gain deviation was minimized in the 1560 - 1610 nm wavelength range. The chromatic dispersion was around -100 to -140 ps/nm/km for the EDTFAs and -10 to -100 ps/nm/km for the EDSFAs.

Eight polarization-aligned CW signals with a 100 GHz spacing from 1572 to 1583 nm were launched into the EDFAs to measure the FWM light generated in the EDFAs. Figure 13 shows the output spectra of samples A and D when the signal input power was -11 dBm/ch⁽¹⁴⁾. FWM light was observed at 1579 nm. The FWM light power was much smaller in sample D which had a larger mode field diameter (MFD) and erbium concentration. Figure 14 shows the ratio between the signal power and FMW light power when the input signal power was changed⁽¹⁴⁾. The signal gain was kept at 25.5 dB by controlling the pump power. It was found that the FWM is more serious in EDTFAs than in EDSFAs. However, the large FWM in EDTFAs was suppressed to almost the same degree as that generated in EDSFAs by expanding the MFD to 7.5 μm and shortening the EDTF length by increasing the erbium

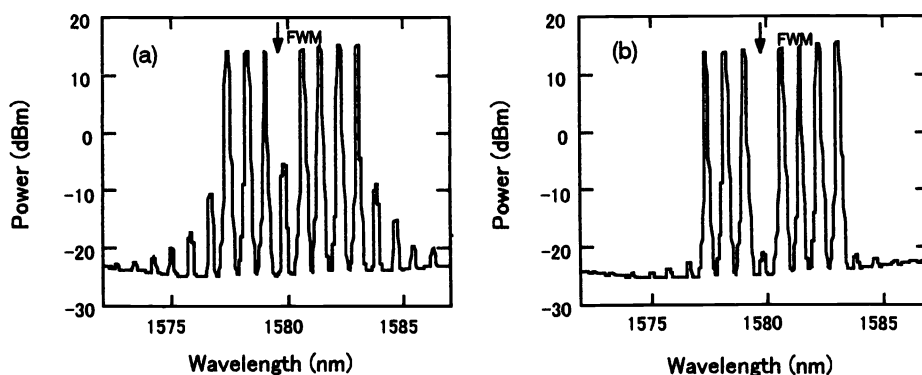


Figure 13 Output spectrum EDTFA : (a) sample A and (b) sample D

concentration to 2000 ppm.

Expanding the MFD to 7.5 μm reduced the PCE by 20 - 30 % in the small signal region, but the PCE difference was small in the saturation region. In addition, the PCE degraded only slightly when the erbium concentration was increased to 2000 ppm. Expanding the MFD and increasing the erbium concentration were effective ways to suppress the FWM phenomenon in EDTFAs.

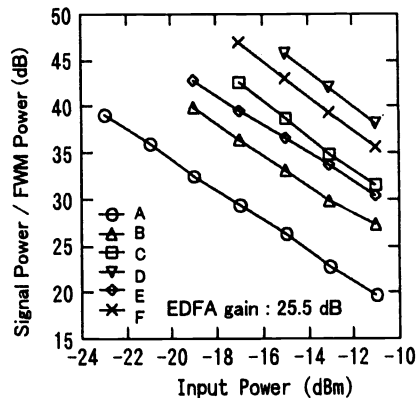


Figure 14 Power ratio between output signal and FWM

4. BROADBAND FIBER RAMAN AMPLIFIER TECHNOLOGY

In early demonstrations of transoceanic and ultra-long-haul terrestrial WDM transport systems, FRA has been used together with EDFA to increase the un-regenerated system reach. However, improved performance has recently been achieved only using FRA. It is desirable in this case that the amplification bandwidth is as broad as possible. Multi-wavelength pumping is a powerful way to realize broadband and flat Raman gain spectra⁽¹⁵⁾. A 80 nm gain bandwidth has been achieved using silica-based FRM for discrete-type in-line repeater application⁽¹⁵⁾.

It has been reported that tellurite-based fiber is a promising candidate for an amplification medium of ultra-broadband FRA⁽¹⁶⁾. Figure 15 shows the gain coefficient spectra of (a) tellurite-based and (b) silica-based fiber⁽¹⁶⁾. The peak gain coefficient for the tellurite-based fiber is $55 \text{ (W}^{-1}\text{km}^{-1}\text{)}$. It is 16 times larger than that of the silica-based fiber. The Stokes shift of the gain is 170 nm for the tellurite-based fiber. It is 1.7 times larger than that of 100 nm for the silica-based fiber. In addition, the tellurite-based fiber has a twin-peaked spectrum, while the silica-based fiber has a single peak as well known. This means that the tellurite-based has a potential for realizing a broader Raman gain spectrum than the silica-based fiber. Figure 16 shows the configuration and gain characteristics of the tellurite-based FRA⁽¹⁶⁾. The total pump power is 1,090 mW using four-wavelength-channel pumping LDs. A small signal gain of over 10 dB has been obtained in the 160 nm bandwidth from 1490 to 1650

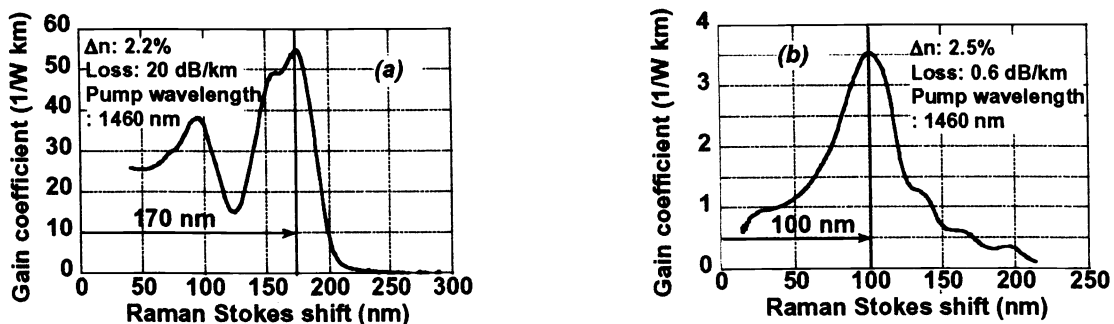


Figure 15 Raman gain coefficient spectra
(a) Tellurite-based fiber (b) Silica-based fiber

nm. The noise figure is less than 10 dB. The tellurite-based fiber is an attractive gain medium for ultra-broadband amplification.

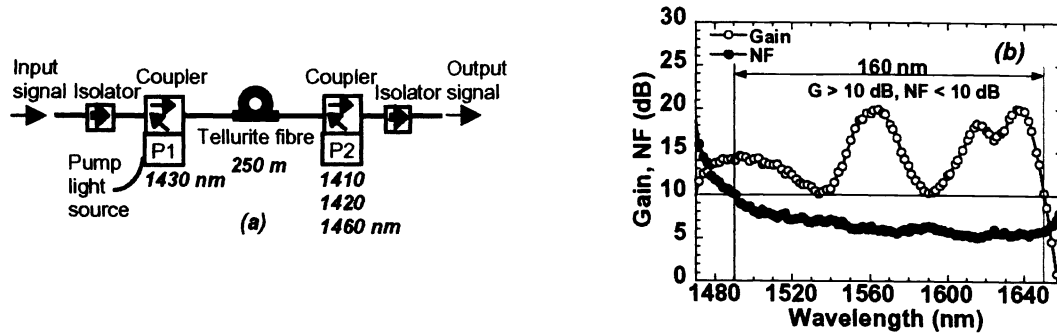


Figure 16 Multi-wavelength pumped tellurite-based FRA
 (a) Configuration (b) Small signal gain and noise figure spectra

5. Prospect of bandwidth expansion of optical fiber amplifiers

After the emergence of EDFAs, various rare-earth-doped fiber amplifiers and FRA have been developed in this decade in order to expand operational bandwidth of optical fiber amplifiers. The operational band of EDFAs has been expanded from the C-band to S⁽⁷⁾- and L-band. Wideband EDFAs which cover both C and L-band have been developed by adapting tellurite-based fiber as a new erbium host.

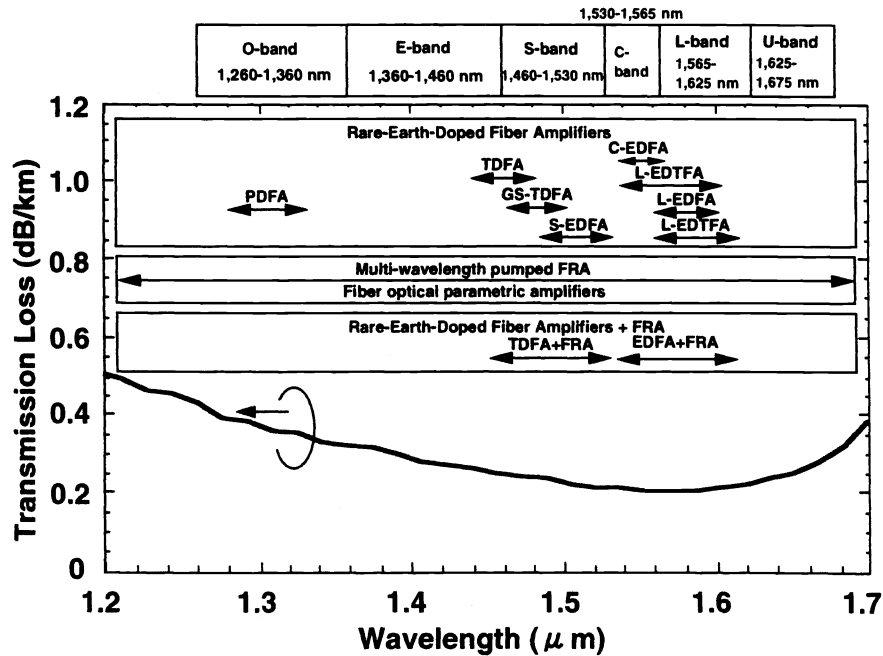


Figure 17 Gain spectra of various optical fiber amplifiers

Thulium has been used as an active ion for amplification in the S-band. The usable bandwidth of the DWDM transmission systems has been expanded from the S- to L-band by using these rare-earth-doped fiber amplifiers as shown in Figure 17. But, it is essentially difficult to expand the 4f - 4f transition bandwidth drastically by changing rare-earth hosts. Further bandwidth expansion can be performed only by combining each amplification band when we use rare-earth-doped fibers as amplification media.

The operational band of FRA depends on the pump wavelength and is more flexible compared with rare-earth-doped fiber amplifiers. A broadband FRA with a bandwidth of more than 200 nm has been realized by a multi-wavelength pumping⁽¹⁷⁾. FRA is a promising candidate as ultra-broadband optical amplifiers. Furthermore, when they are operated as distribution amplifiers, they are effective in improvement of SNR for the transmission systems. They have become popular devices especially for the long haul transmission systems, though the pump efficiency is much lower than EDFAs.

A hybrid operation of FRA and rare-earth-doped amplifiers is a way of expanding the bandwidth of rare-earth-doped optical amplifiers. Hybrid operations of EDFA and FRA, and TDFA and FRA have been performed and their effectiveness to the optical systems has been demonstrated.

OPA is another candidate of ultra-broadband amplifiers. Technical issues of this amplifier are to improve gain efficiency. High nonlinear silica fibers with controlled dispersion characteristics to achieve phase matching condition have been developed. A signal gain of 49 dB has been demonstrated using a high nonlinear silica fiber⁽¹⁸⁾. The bandwidth of 208 nm has been obtained using pulse laser pumping⁽¹⁹⁾. This fiber amplifier is a quite interesting as a candidate of ultra-broadband fiber amplifiers of the next generation. Gain media with much improved nonlinear performance and wavelength dispersion characteristics are required to make OPA practical devices in the optical systems. An OPA has been designed using a heavy metal oxide glass as a fiber material⁽²⁰⁾. This would be another research trend to make OPA a practical device in optical telecommunication systems.

6. CONCLUSION

The development status of rare-earth-doped fiber amplifier, FRA and OPA technology has been reviewed here. Rare-earth-doped fiber amplifiers technology will increasingly mature and spread its application field. FRA and OPA are attractive as ultra-broadband amplifier. Steady progress has been made to demonstrate the ultra-broadband potential of FRA and OPA over the past several years. They will find the actual application fields in the optical telecommunication technology after remaining engineering issues. They will play an important role as key devices as well as rare-earth-doped fiber amplifiers to construct ultra-high capacity DWDM transmission systems.

ACKNOWLEDGEMENTS

The results presented in this paper were obtained by the research and development group of NTT Photonics Laboratories and NTT Electronics Corporation. I am sincerely grateful to all the members for their contribution.

REFERENCES

- (1) T. Komukai, T. Yamamoto, T. Sugawa, and Y. Miyajima, "Upconversion pumped thulium-doped fluoride fiber and laser operating at 1.47 μm ," IEEE J. of Quantum Electronics 31, pp. 1880-1889, 1995.
- (2) T. Sakamoto, S. Aozasa, T. Kanamori, K. Hoshino, and M. Shimizu, "Gain-equalized thulium-doped fiber amplifiers for 1460 nm-band WDM signals," in Tech. Dig. OAA'99, WD2, 1999.
- (3) T. Kasamatu, Y. Yano, and H. Sekita, "Novel 1.50- μm band gain-shifted thulium-doped fiber amplifier by using a dual wavelength pumping of 1.05 μm and 1.56 μm ," in Tech. Dig. OFC'99, PDP1, 1999.
- (4) T. Sakamoto, S. Aozasa, T. Kanamori, K. Hoshino, and M. Shimizu, "High gain and low noise TDFA for 1500 nm band employing novel high concentration doping technique," in Tech. Dig. OFC'00, PDP4, 2000.
- (5) S. Aozasa, H. Masuda, H. Ono, T. Sakamoto, T. Kanamori, Y. Ohishi, M. Shimizu, "1480-1510 nm-band Tm doped fiber amplifier (TDFA) with a high power conversion efficiency of 42 %," in Tech. Dig. OFC'01, PDP1, 2001.
- (6) J. M. Thomas, D. Crippa, and A. Maroney, "A 70 nm wide S-band amplifier by cascading TDFA and Raman fibre amplifier," in Tech. Dig. OFC'01, WDD9, 2001.
- (7) E. Ishikawa, M. Nishihara, Y. Sato, C. Ohshima, Y. Sugawa, and J. Kumasako, "Novel 1500 nm-band EDFA with discrete Raman amplifier," in Proc. ECOC'01, PD.A.1.2 2001.
- (8) T. Segi, T. Aizawa, T. Sakai, and A. Wada, "Silica-based composite fiber amplifier with 1480-1560 nm seamless gain-band," in Proc. ECOC'01, Tu.L.3.3, 2001.
- (9) R. Reisfelt, and C. K. Jorgensen, Laser and Excited States of Rare Earths (Springer-Verlag, New York, 1997), Chap.2.
- (10) J. S. Wang, E. M. Vogel, and E. snitzer, "Tellurite glass: a new candidate for fiber devices," Opt. Mater., 3, pp. 187-203, 1994.
- (11) Y. Ohishi, A. Mori, M. Yamada, H. Ono, Y. Nishida, and K. Oikawa, "Gain characteristics of tellurite-based erbium-doped fiber amplifiers for 1.5- μm broadband amplification," Opt. Lett., 23, pp. 274-276, 1998
- (12) A. Mori, T. Sakamoto, K. Kobayashi, K. Shikano, K. Oikawa, K. Hoshino, T. Kanamori, and M. Shimizu, "A 50 nm broadband tellurite-based EDFA with a 0.6 dB gain excursion and a 25.3 dB gain for 1.58 μm -band WDM signals," in Tech. Dig. ECOC'98, I, pp. 268-269, 1998.
- (13) A. Mori, T. Sakamoto, K. Shikano, K. Kobayashi, K. Hoshino, and M. Shimizu, "Gain flattened Er^{3+} -doped tellurite fibre amplifier for WDM signals in the 1581-1611 nm wavelength region," Electron. Lett., 36, pp. 621-622, 2000.
- (14) T. Sakamoto, A. Mori, K. Hoshino, K. Shikano, and M. Shimizu, "Suppression of nonlinear effects in tellurite-based EDFAs fiber parameter modification," in Tech. Dig. OFC'01, TuI6, 2001.
- (15) Y. Emori, "Ultrabroadband fiber Raman amplifiers," in Tech. Dig. ECOC'02, S3.2, 2002.
- (16) A. Mori, H. Masuda, and M. Shimizu, "Ultra-wide band tellurite-based fibre Raman amplifiers," in Tech. Dig. ECOC'02, S3.1, 2002.
- (17) T. Tanaka, K. Torii, M. Yuki, H. Nakamoto, T. Naito, and I. Yokota, "200-nm bandwidth WDM transmission around 1.55 μm using distributed Raman amplifier," in Tech. Digest ECOC'02, PDP4.6, 2002.
- (18) J. Hansryd, and P. A. Andrekson, "Broad-band continuous-wave-pumped fiber optical parametric amplifier with 49-dB gain and wavelength-conversion efficiency," IEEE Photon. Technol. Lett., 13, pp.194-196, 2001.
- (19) M. C. Ho, M. E. Marhic, Y. Akasaka, and L. G. Kazovsky, "Fiber optical parametric amplifier and wavelength converter with converter with 208 nm gain bandwidth," in Tech. Dig. CLEO'00, CThC6, 2000.
- (20) E. S. Hu, Y. L.Hsueh, M. E. Marhic, and L. G. Kazovsky, "Design of highly-nonlinear tellurite fibers with zero dispersion near 1550 nm," in Tech. Dig. ECOC'02, 3.2.3, 2002.